Integrated Active Antenna with Full Duplex Operation

Martin J. Cryan, *Member, IEEE*, Peter S. Hall, *Senior Member, IEEE*, S. H. (Kenneth) Tsang, and Jizhang Sha, *Member, IEEE*

***Abstract*—This paper discusses the design and implementation of a novel two-element active transmit–receive array using dual linear polarization and sequential rotation. Each element includes an integrated oscillator and amplifier mounted on orthogonal edges of a square patch, such that the transmit and receive paths are isolated and polarization duplexed. The array gives in excess of 45-dB transmit–receive isolation with an output power of 5.4 dBm and a receive gain of 8.2 dB at 4.05 GHz. Link budget calculations are used to show expected system performances. These active antennas have potential uses in both short-range communication and radar systems.**

***Index Terms*—Active antennas, antennas, quasi-optics.**

I. Introduction

AN ACTIVE antenna integrates an active device into a printed antenna to improve its performance or combine functions within the antenna itself. Such antennas are of increasing interest [1] as system designers require more complex functions to be implemented in reduced space. New high-volume millimetric applications such as vehicle collision-avoidance radar, wireless local-area networks (WLAN's), and electronic tagging are driving costs lower and putting further constraints on size and weight. This paper hopes to address these demands by taking further steps in the integration of active antennas by combining both transmit and receive functions into a single antenna.

This paper uses a square microstrip-patch antenna resonant at 4.0 GHz, with a metal–semiconductor field-effect transistor (MESFET) centrally mounted on the edge of the patch to form an oscillator [2] and another MESFET, configured as an amplifier on the orthogonal edge to act as the first stage in a receiver. The inherent isolation of the center points of orthogonal edges of a square patch is used as the basis for the transmit–receive isolation. This transceiver is linearly polarized with transmit and receive channels on orthogonal polarizations. The channels are of the same frequency, but could be offset depending on the application. A method to improve the isolation of the single patch is that of sequential rotation [3]. Here, the receiver outputs are taken from opposite edges of the two patches and the phases of the direct feed-through signals from transmit to receive are adjusted so that they are 180° out of phase—which upon combining, will cancel. The received signals are forced to be 180° out of phase by the positions of the receiver outputs; thus, when combined they will add in-phase. This method can increase the isolation by 20–30 dB.

Manuscript received February 27, 1997; revised June 20, 1997. This work was supported by the Engineering and Physical Science Research Council under U.K. Research Grant GR/K03760.

The authors are with the School of Electronic and Electrical Engineering, The University of Birmingham, Edgbaston, Birmingham B15 2TT, U.K.

Publisher Item Identifier S 0018-9480(97)07108-1.

II. Results

A. Passive Element

The basis for the transmit–receive isolation is the orthogonal positioning of the oscillator and amplifier. Measurements were carried out to assess the levels of obtainable isolation. These results are shown in Fig. 1. Two sets of results are shown: 0.1-mm-diameter wire bonds across a 0.5-mm gap at the end of a 50-Ω transmission line and quarter-wave transformers from 50 Ω to the patch edge impedance. It is seen that with wire-bond connections very high isolations can be obtained, but with poor match. This appears to be due to the fact that as the width of the launch onto the patch is reduced there are fewer orthogonal currents excited and, hence, fewer orthogonal modes. It is the orthogonal modes which will cause the coupling between the two ports. Thus, a narrower launch produces higher isolation. However, in the case of quarter-wave transformers, the isolation is seen to be the worst at resonance. This seems to be caused by the fact that the patch is highly resonant, and all modes (including orthogonal ones) are more likely to be excited at the resonant frequency. Thus, the isolation is reduced. It may be that a compromise between match and isolation has to be reached in a final system design.

B. Patch Oscillator Design

The critical active element in this system is the microstrip-patch oscillator. The oscillator has been designed using the Hewlett-Packard Microwave-Design System (MDS) harmonic-balance (HB) simulation, and is based on Fusco's design [2]. The basic MDS schematic circuit is shown in Fig. 2. The patch is represented using a transmission-line model [4], the length extension DL and radiation resistance R_R are defined in terms of the physical parameters of the patch using equations within the MDS. The active device is an atf26884 MESFET and is modeled using the built-in large signal model available within MDS. Initially, a small-signal oscillator design is carried out to ensure a negative resistance is present *looking* into the gate port of the oscillator, and that the oscillation frequency is close to that required [5]. This

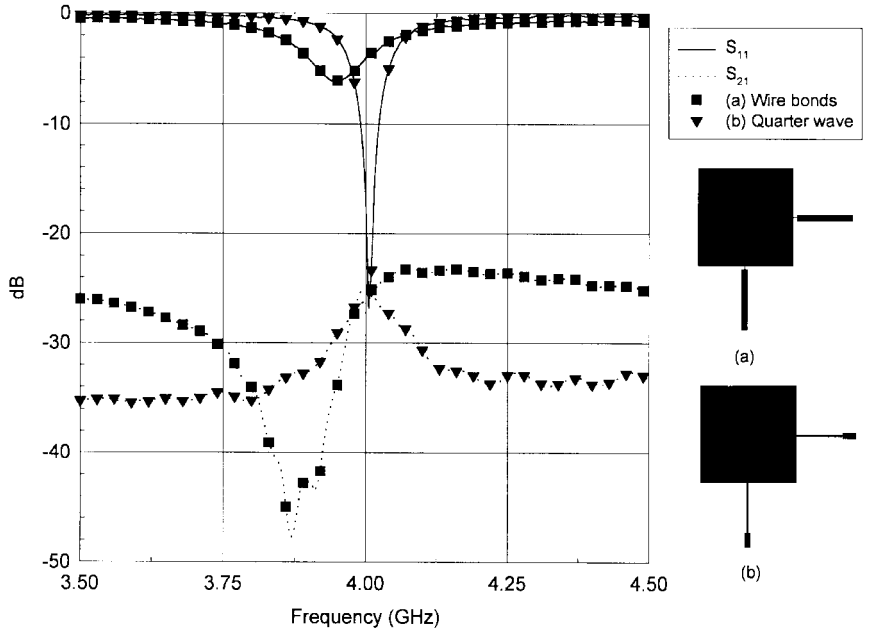

Fig. 1. S-parameters of an orthogonally fed square patch. (a) Square patch with 0.1-mm wire bonds across 0.5-mm gaps. (b) Square patch with quarter-wave transformers. Patch length $(L_{p1} + L_{p2} + L_{p3}) = 24$ mm, width $(W_p) = 24$ mm, 50 Ω width $= 1.55$ mm, $\varepsilon_r = 2.33$, substrate height $= 0.508$ mm.

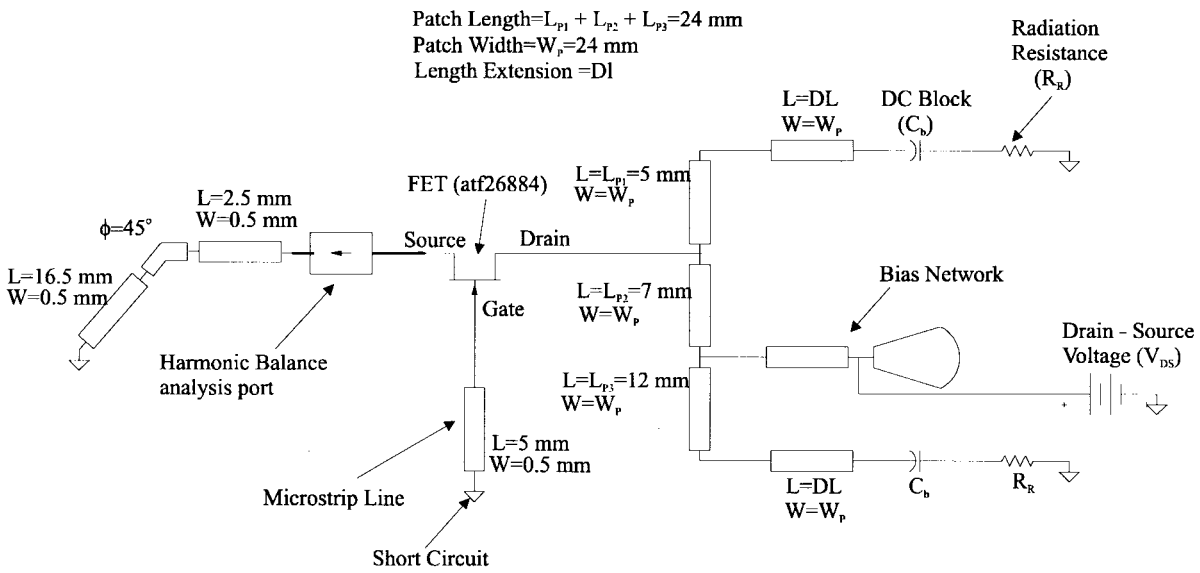

Fig. 2. MDS circuit schematic for HB simulation of a microstrip-patch oscillator.

is followed by a large-signal HB analysis which ensures that oscillation is possible and gives a more accurate estimate of the oscillation frequency and output power.

Fig. 2 shows the schematic layout for the patch oscillator model; the patch is represented by five transmission lines, which allows for the connection of bias circuits and active device. The transistor is connected close to the 50-Ω point on the nonradiating edge of the patch, and short-circuited transmission lines are connected to the source and gate terminals of the FET. Drain bias is applied to the patch via a radial-stub bias circuit. The oscillator free-running frequency can be tuned by altering the drain-bias voltage; this allows the possibility of employing frequency or phase modulation techniques. Fig. 3 shows a schematic generated from Fig. 2 for the physical layout of the patch oscillator circuit.

Measured and modeled results for frequency and output power have been compared, and are shown in Fig. 4. The modeled output power is defined as the sum of the powers in the radiation resistances, and the measured output power has been calculated from the effective isotropic radiated power (EIRP) and the gain of an identical passive array. Fig. 4(a) shows the free-running frequency-tuning response—the trend between measured and modeled results shows reasonable agreement. However, absolute agreement is less good. This will be very dependent on the agreement between the large-signal model and the actual device used, and due to device

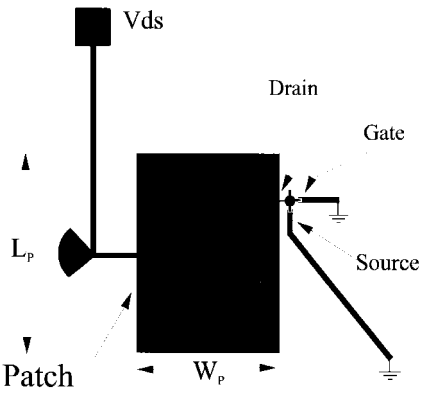

Fig. 3. Physical layout for a 4-GHz patch oscillator. Patch length $(L_p) = 24$ mm, width $(W_p) = 20$ mm, $\varepsilon_r = 2.33$, substrate height $= 0.508$ mm.

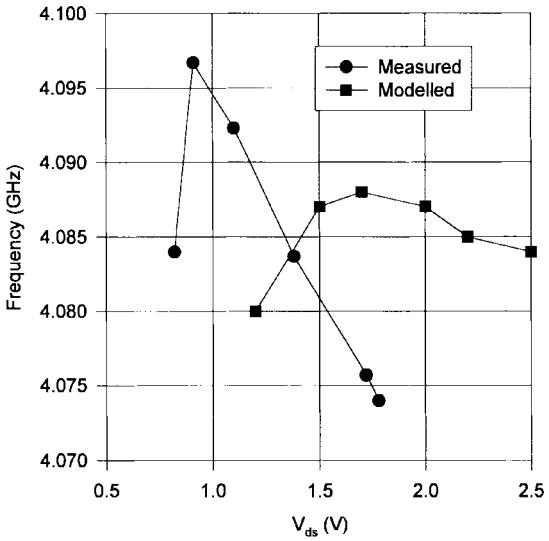

(a)

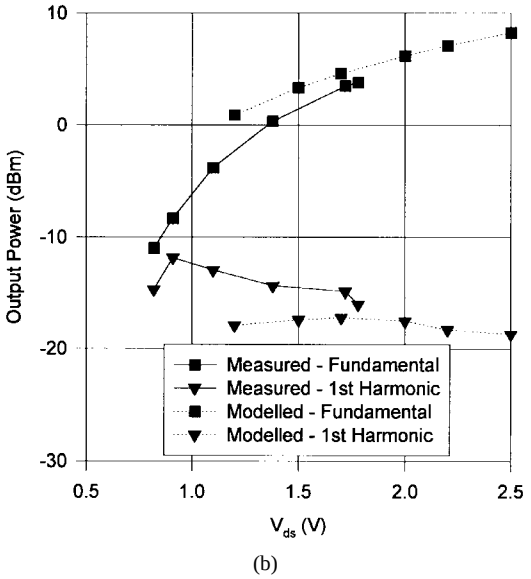

(b)

Fig. 4. Measured and modeled performance of a 4-GHz patch oscillator. (a) Frequency and (b) output power at fundamental and first harmonic. Patch length $= 24$ mm, width $= 20$ mm, $\varepsilon_r = 2.33$, substrate height $= 0.508$ mm.

repeatability this could be quite poor. However, in the range 1.2–1.7 V, the agreement is better than 1%. Fig. 4(b) shows the output power, and good agreement is shown for the fundamental and reasonable agreement for the first harmonic. These results suggest that a voltage-controlled patch oscillator can be designed and implemented to a reasonable level of accuracy by using currently available simulation packages. A tuning range of 20 MHz is achieved, which would be sufficient for many system applications.

III. Active Integrated Antenna–Transceiver Design

A schematic of the array is shown in Fig. 5. Both elements are integrated into one substrate measuring 150 mm $\times$ 190 mm. The circuit has been designed using MDS; measured S-parameter data for the microstrip-patch, FET's, and dc blocks have been imported into MDS in order to obtain high accuracy for the phase-shift networks which are essential for good operation. All FET's are of type atf26884. The patch oscillator is similar to that shown in Fig. 3, but here the patch is 24 mm $\times$ 24 mm and the oscillator is centrally mounted on the patch in order to obtain high isolation, as shown previously. The gate and source stubs are identical to those shown in Fig. 3 and a gate-bias circuit has been added to allow improved tuning of frequency and power output. The amplifier FET is mounted in a 50-Ω transmission line with dc blocks and choke coils for biasing and a wire-bond connection to the patch in order to maintain high isolation. Input and output matching circuits have also been included. An electronic loaded-line phase shifter is included to correct for small differences between the elements.

To form the array, the two elements are spaced by λ_o, the oscillators lock together by mutual coupling, and power combining occurs in the far field. This spacing is required to ensure that the oscillators lock in-phase—spacing of less than $0.75\lambda_o$ have been shown to cause out-of-phase locking of the oscillators [6], which can lead to problems with the sequential rotation technique. This spacing will produce high-level array sidelobes, as will be shown later. However, by using *hard* locking with lengths of transmission lines, smaller spacings can be achieved while maintaining in-phase locking. The outputs from the two amplifiers are connected to a power combiner through 50–100 Ω tapers in order to maintain output matching and the lines have a 180° phase difference at a frequency of 4 GHz. It was found that small differences in

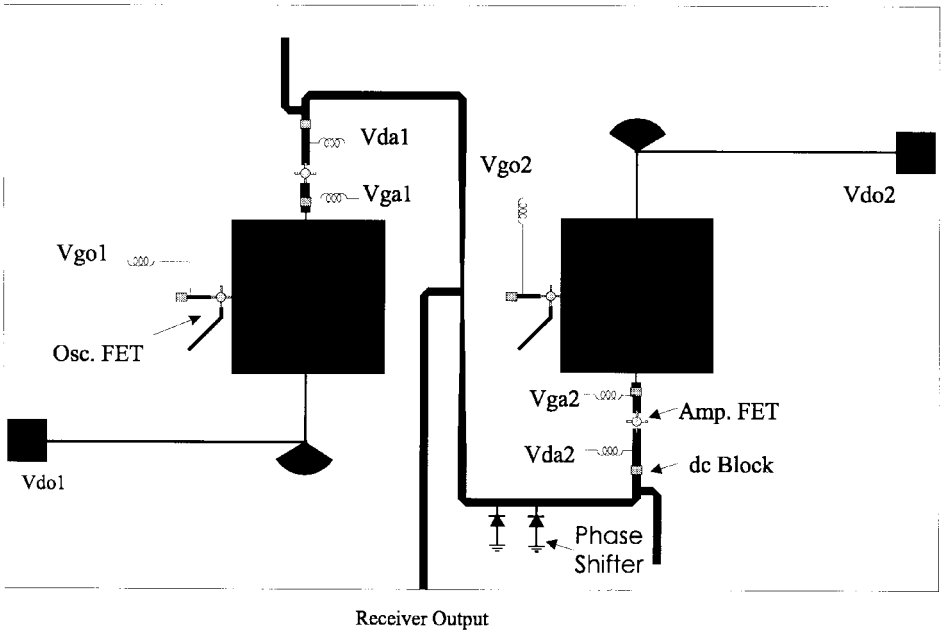

Fig. 5. Sequentially rotated two-element active array. Patch length = 24 mm, width = 24 mm, $\varepsilon_r = 2.33$, substrate height = 0.508 mm.

the wire-bond positions and oscillator output powers produced quite large differences in the isolation signal in the order of 5–10 dB. Final cancellation of the transmit signal breaking through into the receiver was achieved by control of both the phase shifter and the amplifier gains. This highlighted the need for very repeatable elements when employing a phase cancellation method. On receive, the two ports are rotated through 180°. Because of the nature of the TM_{01} mode [4] being used on the patch, the signals will be in antiphase; thus, they will combine in-phase on passing through the combiner network. The measured results are shown in Fig. 6. Fig. 6(a) shows the oscillator output power together with the isolation signal after cancellation. The output power of the oscillator is calculated from the EIRP and measurements of the gain of an identical passive array. Frequency tuning is performed by adjusting both drain and gate voltages of both oscillators. The tuning bandwidth was found to be 28 MHz centered on 4.04 GHz. An array output power of 5.4 dBm was obtained with an isolation of better than 45 dB at 4.05 GHz. The isolation is better than 43 dB across the whole band, and this could be improved by using broad-band constant phase-shift networks, such as Schiffman phase shifters. Fig. 6(b) shows the receive performance. A gain of 8.2 dB was obtained at 4.05 GHz—the maximum being 16.5 dBi. The output return loss is better than 10 dB from 4.04 to 4.20 GHz. The transmit and receive bands are reasonably well aligned, and with minor modifications to the matching networks, an optimum design could be achieved. Initially, it was felt that greater isolation could be obtained since the passive isolation with wire-bond connections was 40 dB, thus with sequential rotation this might be expected to be 70 dB. However, since the amplifier is matched to the patch edge impedance, and the oscillator as a result of the oscillation conditions [5] is delivering all its output power to the patch, then a more realistic estimate for the passive isolation was that of the quarter-wave matched patch. This agrees with the results of Fig. 6, since with a passive isolation of 25 dB from Fig. 1(b) and an extra 30 dB from sequential rotation, the overall isolation would be approximately 55 dB—similar to that shown in Fig. 6. These results suggest that by mismatching the amplifier, extra passive isolation could be achieved at the expense of receiver gain. Further work is required to quantify this effect.

The radiation patterns have been measured and are compared with theoretical predictions assuming passive patches. The results are shown in Fig. 7. Fig. 7(a) and (b) show the E- and H-planes receive patterns, respectively. Good agreement with theoretical passive patch patterns has been obtained. The receive H-plane pattern is shown in Fig. 7(b), with the array sidelobes discussed earlier due to the λ_o spacing observed. Fig. 7(c) and (d) show the transmit E- and H-planes, respectively. Reasonable agreement is shown in both cases. These measurements were found to be difficult to perform due to the sensitivity of the oscillators' mutual locking to physical movement. Fig. 7(c) shows a shift of the boresight by approximately 15°. This is due to the inter-element phase shift that can be introduced if both oscillators do not have exactly the same free-running frequency [7]. However, good general agreement is shown with the sidelobe levels being well predicted.

IV. System Performance

It is envisaged that larger arrays of the type discussed above could be used in communication systems. A typical array is shown in Fig. 8. One of the main advantages of active arrays can be seen here, in that only a receive feed network is required, the transmit combining occurs in free space, greatly reducing the array complexity and feed losses. Another advantage of an active array is that as the array size grows, not only is the gain increased, but also the total output power increases as each element is added. This will be quantified

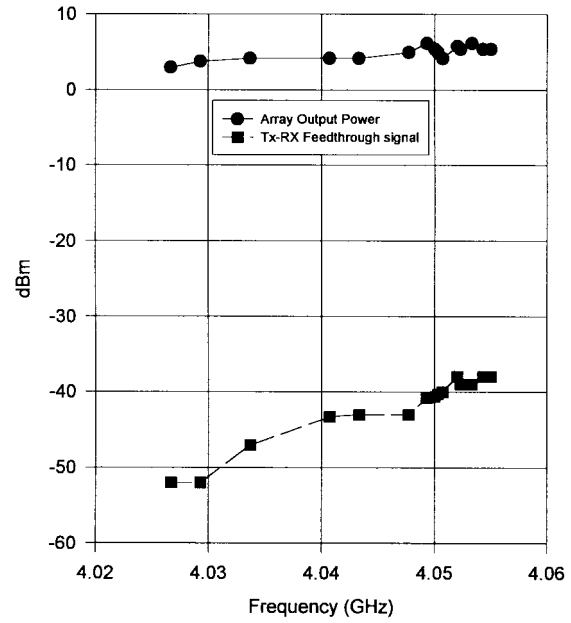

(a)

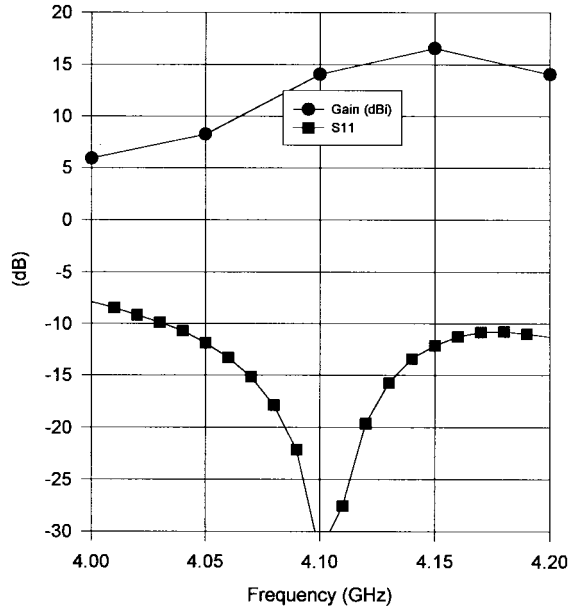

(b)

Fig. 6. Results for array shown in Fig. 5. (a) Transmit. (b) Receive.

in more detail by the system calculations that follow. The reliability of active arrays can also be greater than conventional single-transmitter systems since the failure of one active device in the array does not mean the failure of the whole system. Modulation schemes could included both frequency and phase-shift keying since the free-running frequency of the oscillators can be tuned over tens of megahertz by control of the oscillator bias voltages, and injection-locking techniques [7] allow control of the oscillator phase. The system could be further integrated by including more of the receiver in the array. Mixers could be directly included onto the substrate with a stable local-oscillator signal fed to each mixer to preform downconversion. Fig. 8 does not show amplifiers included in the system (as in the array of Fig. 5), and it is not clear as to the most efficient distribution of amplifiers within the system. It may be that the optimum use of amplifiers is with groups of four elements rather than at every element. Further work is required to obtain the optimum design.

V. Link Budget Calculation

Link budget calculations have been carried out in order to assess the size of the array that would be necessary for a given range requirement. The calculations assume that the system is limited by the isolation signal level and not the receiver noise. The link budget calculations will be based on a typical signal-to-noise ratio (SNR) of 10 dB. In the following analysis, an expression for the SNR in terms of range will be calculated.

Let $P_i =$ output power from the ith element and $G_i =$ gain of the ith element (transmit or receive); therefore, the EIRP of the ith element is

$$E_i = P_i G_i. \tag{1}$$

The total EIRP is then

$$E_T = N^2 P_i G_i \eta_c \tag{2}$$

where N is the number of elements in the array and η_c is the combining efficiency. The total receive gain is given by

$$G_{RT} = N G_i G_A L_f \eta_c \tag{3}$$

where G_A is the gain of the receive amplifier and L_f is the total receive feed loss.

Using the Friis formula, we can write an expression for the total received power P_R as follows:

$$P_R = E_T G_{RT} \left(\frac{\lambda_0}{4\pi d}\right)^2 \tag{4}$$

where d is the propagation range. Substituting (2) and (3) into (4), we obtain

$$P_R = N^3 P_i G_i^2 G_A L_f \eta_c^2 \left(\frac{\lambda_0}{4\pi d}\right)^2. \tag{5}$$

The power leaking from the transmit oscillators into the receive port is

$$P_{\text{iso}} = \frac{N}{2} P_i I_{\text{pas}} I_{\text{seq}} G_A L_f \tag{6}$$

where I_{pas} is the isolation of the passive element and I_{seq} is the extra isolation obtained from sequential rotation. The factor 2 occurs because an isolation of $I_{\text{pas}} I_{\text{seq}}$ relates to pairs of elements.

Assuming that the transmitter leakage is the dominant noise contribution, the ratio of (5) to (6) gives the SNR. At this point, fade margin (M_f) can be included in the calculation to allow for variations in the propagation channel caused by atmospheric effects. The final expression for the SNR, R, is

$$R = 2N^2 G_i^2 \eta_c^2 \left(\frac{\lambda_0}{4\pi d}\right)^2 \frac{1}{I_{\text{pas}} I_{\text{seq}} M_f}. \tag{7}$$

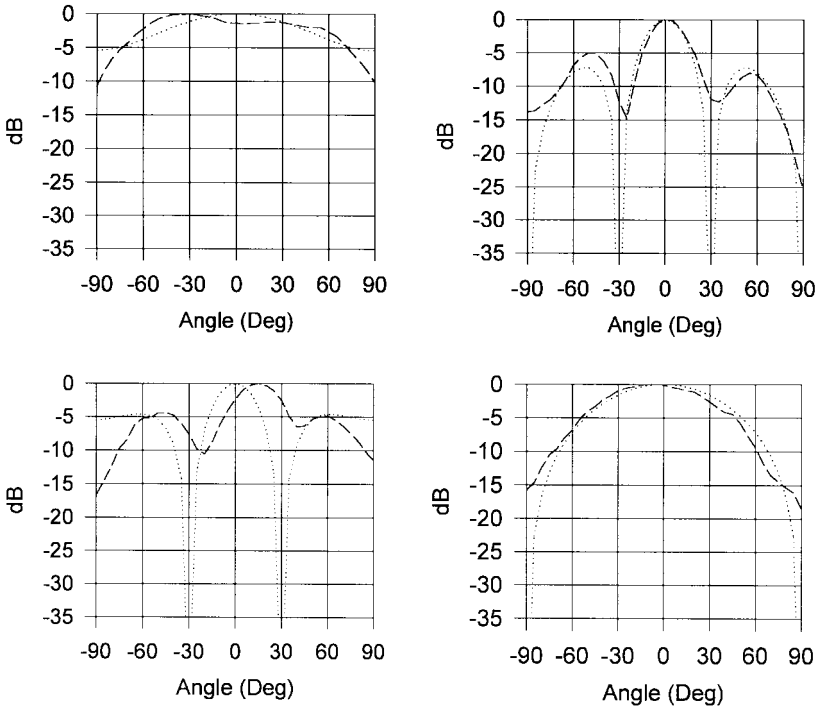

Fig. 7. Measured (— — —) and theoretical (· · · · · · · · ·) transmit and receive radiation patterns for the array of Fig. 5.

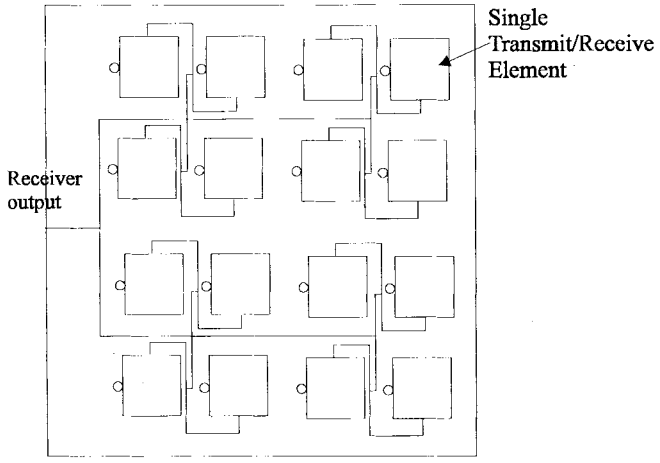

Fig. 8. A schematic of a 4 × 4 active array used in a full duplex communication system.

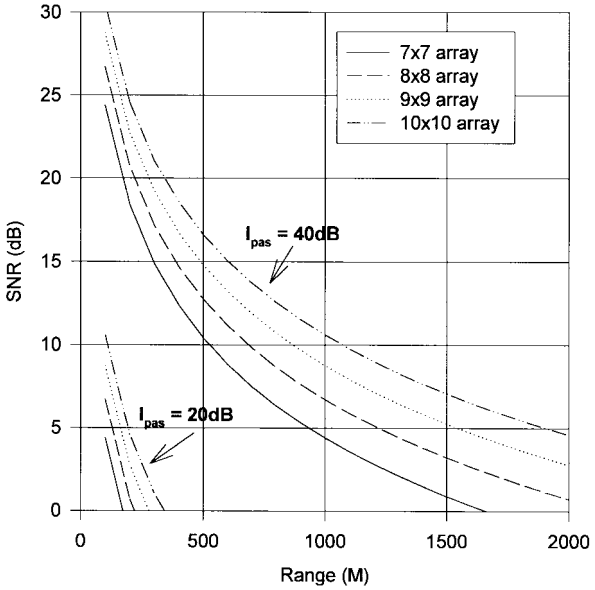

Fig. 9. System range calculations for an active integrated array operating at 4.0 GHz with $\eta_c = -0.45$ dB, $G_i = 6.5$ dB, $I_{\text{seq}} = 30$ dB, and $M_f = 10$ dB.

Equation (7) shows that R is independent of the amplifier gains and feed losses. This equation has been evaluated with typical system parameters and is plotted in Fig. 9 for different array sizes. Fig. 9 shows that with a passive isolation of 40 dB, a 10 × 10 array will give ranges of 1 km with an SNR of 10 dB and a fade margin of 10 dB. Since the SNR is independent of the receive amplifier gain, the amplifier can be mismatched, as discussed earlier, in order to increase the passive isolation from 20 dB. For operation at higher frequencies in the millimeter-wave bands, larger arrays will be required in order to overcome the increased free-space loss. However, at these frequencies, ranges are expected to be much shorter, typically hundreds of meters. In the millimeter bands, since the wavelength is much shorter, the physical size of the array will be reduced and either partial or even full monolithic integration of the array becomes feasible. Using monolithic technology, larger arrays should present fewer manufacturing difficulties since the whole array, including active devices and feed networks, could be produced in one process run—and increased element-to-element repeatability should produce better system performance.

VI. Conclusion

A novel simultaneous transmit–receive active array has been described using dual linear polarization and sequential rotation

to achieve very high values of transmit–receive isolation. The sequential rotation technique, while leading to increased isolation, has been found to require very repeatable active patches, which can be difficult to achieve in practice. A best-case transmit–receive isolation of 45 dB has been obtained with an array output power of 5.4 dBm. These results show the possibility of using larger arrays of this type in the millimetric bands for short-range communication or radar systems. At these frequencies, the advantages of quasi-optical power combining and no feeder losses on transmit make this a viable alternative to conventional single-transmitter systems. Furthermore, the use of millimeter-wave monolithic integrated circuits would enable the technique presented in this paper to be implemented with high repeatability, at very low cost, and in large volumes.

REFERENCES

[1] T. Itoh, "Quasi-optical microwave circuits for wireless applications," *Microwave J.*, vol. 38, no. 1, pp. 64–85, Jan. 1995.

[2] V. F. Fusco, "Series feedback integrated active microstrip antenna synthesis and characterization," *Electron. Lett.*, vol. 28, no. 1, pp. 89–90, Jan. 1992.

[3] P. S. Hall, "Dual circularly polarized sequentially rotated microstrip array with high isolation," *Microwave Opt. Technol. Lett.*, vol. 5, no. 5, pp. 236–239, May 1992.

[4] J. R. James, P. S. Hall, and C. Wood, *Microstrip Antenna Theory and Design.* Stevenage, U.K.: Peregrinus, 1981.

[5] K. Kurokawa, "Injection locking of microwave solid-state oscillators," *Proc. IEEE*, vol. 61, pp. 1386–1410, Oct. 1973.

[6] D. E. J. Humphrey, "Eigenvalue mode confirmation in a mutually coupled active antenna chain array," in *26th European Microwave Conf.*, Prague, Czech Republic, Sept. 1996, pp. 614–617.

[7] A. Zarroug, P. S. Hall, and M. Cryan, "Active antenna phase control using subharmonic locking," *Electron. Lett.*, vol. 31, no. 11, pp. 842–843, May 1995.

Martin J. Cryan (S'91–M'95) was born in Birmingham, U.K., in 1965. He received the B.Eng. degree from the University of Leeds, Leeds, U.K., in 1986, and the Ph.D. degree from the University of Bath, Bath, U.K., in 1995.

From 1986 to 1991, he worked as a Microwave Design Engineer in the fields of microwave integrated-circuit design and waveguide component design. Since 1994, he has been an EPSRC Research Fellow with the Communication Engineering Group, School of Electronic and Electrical Engineering, The University of Birmingham, Birmingham, U.K. In 1988, he received a joint patent for work on stripline attenuators. His research interests include modeling and measurement of microwave and millimeter-wave circuits—in particular active antennas and GaAs MMIC's, and is involved in a research project entitled "New Configurations for Planar Active Antennas."

Peter S. Hall (M'88–SM'93) received the Ph.D. degree in antenna measurements from Sheffield University, Sheffield, U.K., in 1973.

From 1974 to 1976, he was with Marconi Space and Defense Systems, Stanmore, U.K., working largely on a European communications satellite project. In 1976, he joined The Royal Military College of Science as a Senior Research Scientist, doing fundamental research on microstrip antennas, and in 1980, he obtained a lecturing post and progressed to Reader in electromagnetics. In 1994, he joined The University of Birmingham, Birmingham, U.K., where he is currently Professor of Communications Engineering and Head of the Communications Engineering Group, School of Electronic and Electrical Engineering. He has published three books, over 90 learned papers, and holds several patents, and his work has attracted numerous research grants and consultancies. He has done extensive research in the areas of microwave antennas and associated components and antenna measurements.

Dr. Hall is a Fellow of the Institution of Electrical Engineering (IEE) (U.K.), chairman of the IEE Antennas and Propagation Professional Group, chairman of the organizing committee of the 1997 International Conference on Antennas and Propagation, and member of the organizing committee of the French International Symposium on Antennas and of the Technical Committee of the 4th International Symposium on Antennas and Electromagnetic Theory in China. He was the honorary editor of *Proceedings IEE–Part H*, from 1991 to 1995, and invited guest editor of a special issue of the *Microwave and Millimeter Wave Computer Aided Design Journal*. He has received six IEE Premium Awards, including the 1990 IEE Rayleigh Book Award for the *Handbook of Microstrip Antennas*.

S. H. (Kenneth) Tsang was born in Hong Kong, in 1974. He received the B.Eng. degree from The University of Birmingham, Birmingham, U.K., in 1996, and is currently working toward the Ph.D. degree in the Communication Engineering Group, School of Electronic and Electrical Engineering.

His research interests include the technology of vehicle and automotive radar systems.

Jizhang Sha (M'97) was born in China, in 1943. He received the Dip.Eng. degree from Xi'dian University, Xi'dian, China, in 1965.

From 1965 to 1992, he was a Lecturer and Head of the group investigating pulsed radar systems at Xi'dian University. In 1992, he joined Hehai University as Associate Professor in the Department of Electronic Engineering, and became the Head of the group investigating the transmission and processing of television signals. In 1996, he joined The University of Birmingham, Birmingham, U.K. He has authored over 20 publications and has two books on high-frequency electronic circuits and television technology.

Dr. Sha was awarded an Honorary Research Fellowship at The University of Birmingham, in 1996.